Experimental analysis of intermodulation distortion and error vector module for multitone RoF-OFDM system

KULWINDER SINGH[a], KAMALJIT SINGH BHATIA[b,*], HARDEEP SINGH RYAIT[c]
[a]*ECE Department, BMS College of Engineering, Sri Muktsar Sahib, India*
[b]*ECE department, GB Pant Institute of Engineering & Technology, Pauri Garhwal, India*
[c]*Canadian Center of Behavioral Neuroscience, Univ. of Lethbridge Canada*

In this work, we report modeling and performance investigation of OFDM based Radio over Fiber (RoF) system with different tone signals to combat the different distortions like Intermodulation Distortion (IMD) and Error Vector Module (EVM) etc. It is observed that for low value of RF tone amplitude, the intrinsic IMD3 components are quite small as compared to the fundamental components. But as the amplitude is increased to high value, the IMD3 amplitudes become greater than fundamental components. Optimum value of modulation index is calculated at which fundamental power and IMD3 power becomes equal. We also investigate EVM for three types of modulations (4QAM, 16QAM & 64QAM) against different parameters like SSMF length, MZM bias, drive power and modulation index etc.

(Received May 25, 2019; accepted February 17, 2020)

Keywords: Multicarrier Modulation, Intermodulation Distortion (IMD), Error Vector Module (EVM), Mach-Zhender Modulator (MZM)

1. Introduction

A Multi-carrier system is a preferable system for growing high data rate and high speed demands because it can efficiently utilize the fiber bandwidth capacity. A multitone RoF system employing a central station (CS) and a remote antenna station (RAS) was tested for direct and external modulation schemes. A small power penalty was reported between the two schemes [1]. Radio over Fiber (RoF) linked small cell network is proposed that is advantageous in providing small power base station with small cost and self organization. Very low power budget (3.75 dBm) is achieved that help in reducing transmission power thus supporting green concept [2]. A new multi-tone test signal generation method was suggested with different frequency tones that employed OFDM (orthogonal frequency-division multiplexing) and spread spectrum (SS) techniques for allowing signal parameters to users with a great flexibility [3]. A new scheme based on orthogonal frequency-division multiplexing (OFDM) technique was developed for producing multiple frequency tones with fine resolution and low design cost [4]. OFDM combined with Fast Fourier Transform (FFT) provided improved performance in terms of power, speed and area but PAPR compensation is not achieved. PAPR improvement is achieved by combining Discrete Wavelet Transform (DWT) with OFDM but at the cost of area overhead [5]. OFDM is common technique for wired and wireless communications but most widely used in optical fiber communication systems. To reduce high PAPR in Optical OFDM systems, Optical Subcarrier Pairing (OSP) technique is proposed. Also to improve OSNR and BER, Subcarrier Exclusion (SE) technique is proposed [6]. For evaluating the channel performance, the effect of multi-tone jitter was evaluated by an analytical bit-error-rate method that was helpful in channel design and optimization [7]. The impact of multi-path interference (MPI) is investigated in RoF network implemented using directly modulated lasers (DMLs). Carrier to noise ratio (CNR) limited by MPI is investigated in terms of signal-to-interference ratio (SIR) [8]. Direct detection (DD) optical OFDM system is investigated in presence of PAPR to measure error vector module (EVM) in QPSK and 16QAM modulation formats on a 400 Km fiber link [9]. Multiband RoF-OFDM system is evaluated for nonlinearity measurement. By properly suppressing nonlinear components, a 7.3% improvement in EVM is observed with proposed technique [10]. RoF applications are investigated with OFDM signal using hybrid photo receiver. A 16% reduction in EVM is achieved with the proposed system [11]. Nonlinear distortions like intermodulation and harmonic distortions induce the error vector module (EVM). To improve the system performance signal to noise distortion ratio (SNDR) is optimized [12]. For a multi band RoF-OFDM system, a new blind equalizer is proposed that can reduce both linear and nonlinear distortions. In the equalizer, third-order intermodulation distortion (IMD) and EVM are observed by distortion mitigation [13]. Various distortions like phase noise, power amplifier nonlinearity and additive noise occur in OFDM. These distortions are quantified by noise power ratio (NPR) and EVM measurements [14]. Nonlinear characteristics like IMD and other intermodulation products (IMPs) can be used to study the effects of clipping on OFDM sampled signals to obtain optimum receiver designs [15]. In multiband RoF-OFDM system, nonlinear inter-modulations (IMs) are investigated between different subcarriers from different channels. To

mitigate these nonlinearities a pre-distortion technique is proposed [16]. A bandwidth scalable OFDM passive optical network (BSOFDM-PON) is proposed to mitigate nonlinearities like IMD aroused in the system by properly adjusting the guard band [17]. Kaur et al. analyzed different modulation distortions such as IMD, CSO and CTB at different frequencies in analog CATV transmission system [18]. OFDM network performance is analyzed using single and double antenna using EVM 5% and EVM 8% conditions. Effect of EVM in terms of bit error rate, frame error rate and block error rate is evaluated for 64QAM system [19]. Nonlinear distortion is mitigated in multiband RoF-OFDM system using frequency separated digital pre-distortion (DPD) model used as a pre-equalizer. Improved signal performance is achieved as EVM is reduced from 6.3% to 3.5% using proposed model [20]. Mode division multiplexed WDM system is investigated using multimode fiber (MMF) with varying parameters like MMF length, data rate and number of users. System performance is observed in terms of Q-factor and bit error rate [21]. 60 GHz RoF-OFDM passive optical network is evaluated using EVM measurements. RF drive power is adjusted at 6dBm to obtain optimum EVM value of 4.8% [22]. Hybrid OFDM-Digital Filter Multiple Access PON system is experimentally investigated using DSP based digital filtering over 25 Km SSMF. Improved EVM performance (> 10dB) is achieved using hybrid OFDM-DFMA PON as compared to standard DFMA PONs [23]. 80 GHz OFDM based radio over free space optics (RoFSO) system is investigated using mode division multiplexing (MDM) technique at varying weather conditions. Significant improvement in terms of signal to noise ratio and total received power is observed with the proposed system [24]. 64QAM-OFDM signal transmissions in 1 to 12 intermediate frequency (IF) channels is experimentally demonstrated over varying length of SSMF. Using proposed model, odd order intermodulation distortions (IMDs) are significantly compressed to provide improved linearity (> 5.4 dB) at acceptable EVM performance [25].

In this paper, after comprehensive literature review of system, we theoretically describe and measure the concept of Multicarrier Modulation. Then experimental cum simulative analysis is made for Multitone RoF-OFDM system based on modulation distortions like third order intermodulation distortions (IMD3) and Error Vector Magnitude (EVM) against RF modulation index of the MZM and their power spectrums results are concluded in the last section.

2. Multicarrier modulation

In Multi-tone modulation, multiple data streams are multiplexed onto a single optical signal. Multi-tone signal is obtained by combining different frequencies (tones), that are applied to the transmitter and at the receiver the detected signal is processed to separate the tones and the data is extracted from each tone. Multi-tone signal is composed of N equally spaced tones that share the common separation Δf. These N tones are identified by a unique frequency as given in the following expression:

$$f_n = f_0 + (n-1)\Delta f \text{ , where n = 1, 2, … , N.} \quad (1)$$

where, f_0 is the lower frequency.

Total number of mixing products is given by expression:

$$M_T = 2NL^2 - 2L^2 + 2L + 1 \quad (2)$$

where, L is the level of mixing. Unique frequencies can be obtained by following expression:

$$f_n = [L(N-1) - N + n + 1]\lambda \quad (3)$$

$$So,\ f_1 = [L(N-1) - N + 2]\lambda \quad (4)$$

$$f_2 = [L(N-1) - N + 3]\lambda \quad (5)$$

$$f_N = [L(N-1) + 1]\lambda \quad (6)$$

For one-tone signal the value of N = 1 and L (Level of mixing) can be chosen as 5 because mixing is significant up to 5 levels. Putting these values in eqn. (2) we get the total number of mixing products = 11. Similarly a two-tone signal mixed up to fifth order, total number of mixing products comes out as 61. And a three-tone signal mixed up to fifth order, total number of mixing products comes out as 111.

In transmission of optical signal the distortion occurs when the signal is deviated from linearity, this distortion is called as intermodulation distortion (IMD). It may be composite second order (CSO) distortion or composite triple beat (CTB) distortion. Non-linearity in the optical signal transmission results in new frequencies such as $f_i + f_j$ and $f_i - f_j$. For, f_1 and f_2 as frequencies of two tones, third order distortion (IMD3) occurs at frequencies of $2f_2 - f_1$ and $2f_1 - f_2$. Also, for three-tone signals having frequencies f_1, f_2 and f_3, third order distortion (IMD3) occurs at frequencies $f_1 + f_2 - f_3$. Assuming the equal power levels of two tones, IMD3 is obtained from the difference of fundamental power & power of third order products

$$IMD3 = P_O - P_{O3} \quad (7)$$

For Optical signal, the fundamental frequency component power (P_{f1}) at a frequency f_1 can be approximated as:

$$P_{f1} = \left[10^{\frac{\alpha L}{10}} L_{att}{}^2 A^2 \Re J_0{}^3(\pi m_{RF}) J_1(\pi m_{RF}) \right]^2 \quad (8)$$

where, $\alpha = 0.2$ dB/Km is the fiber attenuation loss; L = 80 Km is the fiber length; L_{att} = 0.50119 is the attenuation

of the Mach-Zhender modulator; A = 8.65 mW is the amplitude of laser diode; $\Re$ = 0.6 A/W is the responsivity of photodiode; $m_{RF} = \frac{V_{RF}}{V_\pi}$ is the RF modulation index; V_{RF} is the R.M.S voltage of the input RF tones; $J_k(.)$ represents the kth order Bessel function. Also the second fundamental frequency component power P_{f2} at a frequency f_2 is the same as P_{f1}.

Similarly from equation (7), the power of IMD3 component, P_{IMD1} at a frequency of $2f_1 - f_2$ can be calculated as:

$$P_{IMD1} = 2\left(10^{\frac{\alpha L}{10}} L_{att}{}^2 A^2 \Re\right)^2 \left(D_{IM}{}^2 + E_{IM}{}^2\right) \quad (9)$$

$$Where, D_{IM} = \frac{1}{\sqrt{2}}\left\{\begin{array}{l} J_0{}^2(\pi m_{RF}) J_1(\pi m_{RF}) J_2(\pi m_{RF}) \\ \times\left[\cos\left(\theta_{2f1} - \theta_{f2} + \frac{\pi}{4}\right) + \sin\left(\theta_{2f1-f2} - \frac{\pi}{4}\right)\right] \\ -J_0(\pi m_{RF}) J_1{}^3(\pi m_{RF}) \sin\left(\theta_{f2-f1} - \theta_{f1} + \frac{\pi}{4}\right) \end{array}\right\} \quad (10)$$

$$\& E_{IM} = \frac{1}{\sqrt{2}}\left\{\begin{array}{l} J_0{}^2(\pi m_{RF}) J_1(\pi m_{RF}) J_2(\pi m_{RF}) \\ \times\left[\cos\left(\theta_{2f1} - \theta_{f2} - \frac{\pi}{4}\right) - \sin\left(\theta_{2f1-f2} + \frac{\pi}{4}\right)\right] \\ -J_0(\pi m_{RF}) J_1{}^3(\pi m_{RF}) \sin\left(\theta_{f2-f1} - \theta_{f1} - \frac{\pi}{4}\right) \end{array}\right\} \quad (11)$$

Also the angle (θ) at any frequency *(f)* can be calculated by relation as follows:

$$\theta_f = \frac{\pi L D \lambda^2 f^2}{c} \quad (12)$$

where, λ = 1550 nm is the centre emission wavelength of the laser diode; D = 16 ps/nm/km is the chromatic dispersion parameter of the fiber; *c* is the speed of light.

3. Simulation setup

Fig. 1 shows the simulation setup for the Multi tone RoF-OFDM system. Multi-tone RF signal at frequencies $f_1, f_2, \ldots, f_n$ are combined and then split into two parts by an RF splitter. First and second parts are applied to upper and lower electrodes of Mach-Zhender modulator (MZM). First part is applied directly while the second part is applied after passing through a 90° phase shifter. Laser diode is used to emit a 1550 nm continuous-wave optical signal which is applied to MZM. Bias voltage is applied to the upper RF combiner and the lower RF combiner is grounded. When we set the bias voltage to maximum value then only even-order components are generated. But the odd-order components are not completely suppressed because of degradation in extinction ratio of the modulator. The optical signal modulated by MZM is transmitted over 80 km fiber which is then detected by the photo detector and an electrical spectrum analyzer is used to evaluate the received signal. After the distance of 40 km the transmitted signal can be amplified using EDFA and an optical band pass filter (OBPF) is used before the photo detector for reducing the noise due to spontaneous emission.

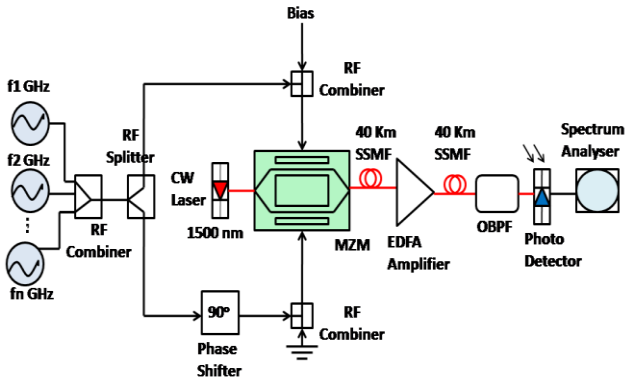

Fig. 1. Simulation Setup for Multi-tone RoF-OFDM System

For the two RF input tones at fundamental frequencies f_1 = 500 MHz and f_2 = 525 MHz, the IMD3 components which are at close proximity to the fundamental frequency components, occur at frequencies equal to $2f_1 - f_2$ and $2f_2 - f_1$. So, the two IMD3 components occur at 475 MHz (2 × 500 – 525) and 550 MHz (2 × 525 – 500).

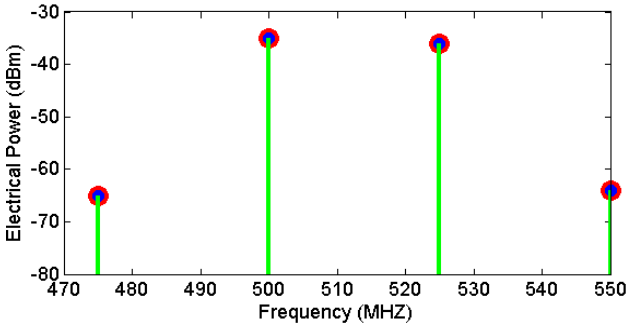

Fig. 2. Two-tone Test for 80 Km SSMF Transmission (RF Tone Amplitude = 1V)

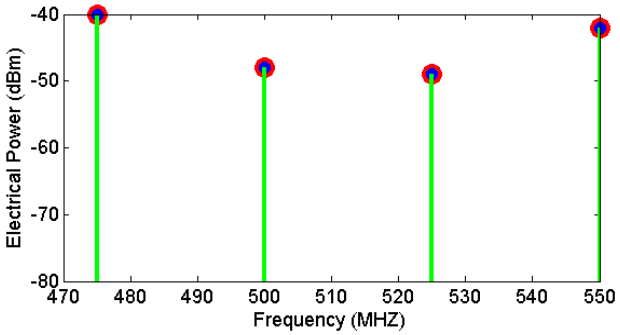

Fig. 3. Two-tone Test for 80 Km SSMF Transmission (RF Tone Amplitude = 3V)

Figs. 2 & 3 depicts the fundamental and IMD3 components with varying RF tone amplitudes. Fig. 2 shows that, for RF tone amplitude = 1V (low value), the intrinsic IMD3 components are quite small as compared to the fundamental components. When RF tone amplitude is increased to 3 (high value), the IMD3 amplitudes become greater than fundamental components (Fig. 3). The fundamental components power and IMD3 components power is computed using equations (8-12).

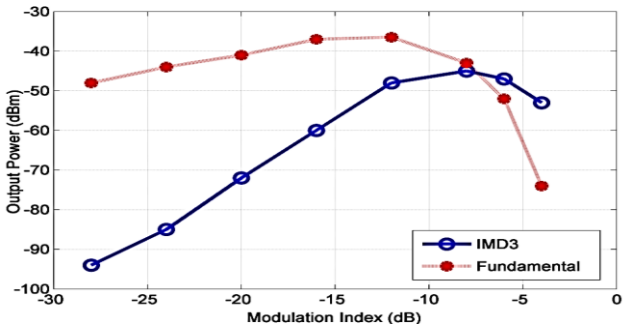

Fig. 4. Variation of Fundamental & IMD3 Powers with Modulation Index

Fig. 4 compares the computed powers of the fundamental and IMD3 components as a function of the RF modulation index of MZM. It is clear that IMD3 power is much lower than that of the fundamental power at low RF modulation index. As the value of RF modulation index increases, the IMD3 power increases faster than the fundamental power. At an optimum value of modulation index, the IMD3 power becomes equal with fundamental power. When RF modulation index is further increased from this optimum value, the IMD3 distortion occurs which degrades the system performance. The optimum value of RF modulation index which is obtained from the analytical approximation comes out to be -7.5 dB.

4. Measurement of Error Vector Magnitude (EVM)

In radio over fiber (RoF) system because of wireless access, the magnitude and phase angle of signal received at the receiver is different from that in transmitter due the fact that the modulation and transmission is non-ideal. As suggested in the Fig. 5, there is a difference between measured vector and reference vector (ideal vector) called as error vector. The error vector magnitude (EVM) measures the signal divergence from an ideal signal i.e. reference signal.

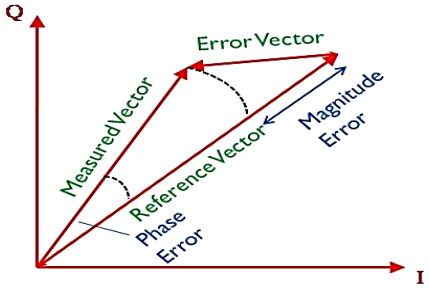

Fig. 5. Error Vector Module

Equation (13) calculates the error vector by subtracting R_n (nth value of received symbol) from I_n (nth value of ideal reference symbol). If a total N OFDM symbols are transmitted then R.M.S value of the EVM (EVM_{rms}) can be obtained from following expression:

$$EVM_{rms} = \sqrt{\frac{\frac{1}{N}\sum_{n=1}^{N}|I_n - R_n|^2}{\frac{1}{N}\sum_{n=1}^{N}|I_n|^2}} \quad (13)$$

EVM_{rms} is also a measure of signal to noise ratio & is related to SNR by equation (14) as

$$EVM_{rms} \propto \sqrt{\frac{1}{SNR}} \quad (14)$$

EVM is widely used parameter for evaluating the quality of system under different conditions. Experimental setup shown in Fig. 6 is used to evaluate EVM for RoF-OFDM system. We consider the optical OFDM signal using three modulation formats i.e. 4QAM, 16QAM and 64QAM. EVM is measured against different parameters such as MZM bias voltage, MZM modulation index, MZM drive power, input power, and fiber length etc. for all three modulation formats.

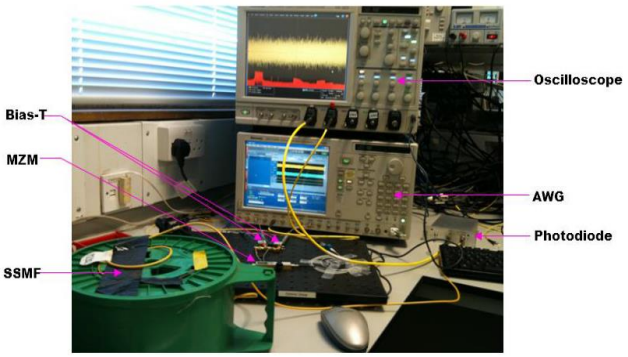

Fig. 6. Experimental Setup to measure EVM in RoF-OFDM System

Fig. 7 provides the constellations for 4QAM, 16QAM and 64QAM modulation formats. From these constellations, we measure the value of EVM against different parameters.

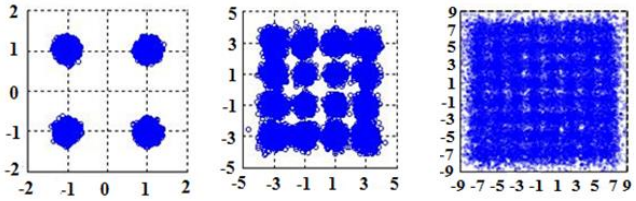

Fig. 7. Constellations for 4QAM, 16QAM and 64QAM Modulation Formats

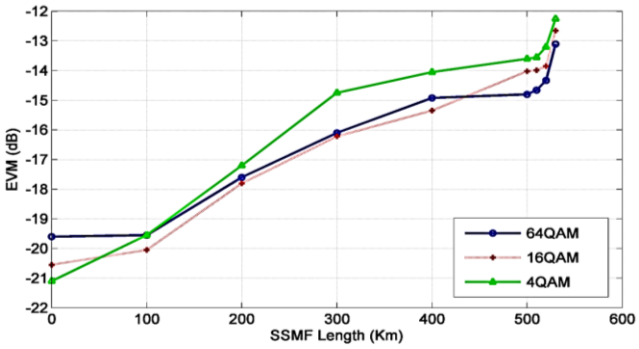

Fig. 8. EVM Degradation with SSMF Length for Different No. of Subcarriers

Firstly, we would like to demonstrate how the system EVM varies with SSMF length for different modulation formats. The SSMF length is varied and the EVM is obtained for each fiber length. This test is repeated for the different modulation formats. Fig. 8 shows the variation of the EVM with the SSMF length for 4QAM, 16QAM and 64QAM formats using the simulation setup of Fig. 1. It can be seen from the figure that as the fiber length is gradually increased, the EVM starts degrading. This is because an increase in the fiber length results in a corresponding increase in the delay spread caused by the fiber chromatic dispersion. The EVM starts degrading when the delay spread exceeds the cyclic prefix length.

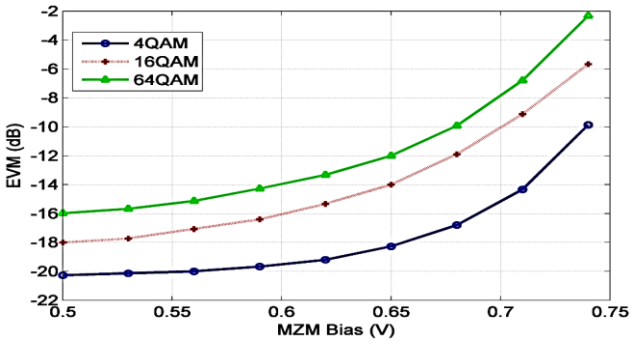

Fig. 9. EVM vs. Normalized Bias for Different Modulation Formats

Fig. 9 examines the OFDM sensitivity against MZM non-linearity for different modulation formats. To do this, the number of OFDM subcarriers is kept fixed at 64 and the modulation format is varied from 4-QAM to 64-QAM. The MZM bias 'ε' is varied from 0.5 to 0.75 for all three modulation formats; and the EVM obtained for each value of ε. Fig. 9 shows the EVM variation with normalized bias for the different modulation formats. It is derived that the system performance against MZM non-linearity is degraded in case of higher modulation formats. For ε = 0.5, the EVM varies from -20.3 dB (for 4-QAM) to -16 dB (for 64-QAM). The amplitudes of the two driving UWB signals are varied and the corresponding values of drive power are measured and the input optical power to the photodetector is fixed at 1 dBm.

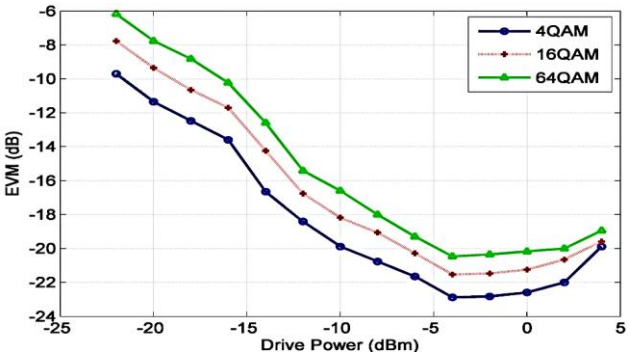

Fig. 10. EVM against Drive Power for Different Modulation Formats

Fig. 10 examines the EVM against UWB drive power for different modulation formats. It is derived that EVM is improved for all the three formats as the drive power is increased from a low value. This is because of the fact that as drive power is increased SNR also increases. This improvement in the EVM continues until the UWB drive power gets to an optimum value of -2 dBm. For UWB power levels greater than -2 dBm, the EVM starts to degrade as the distortion induced by the inherent non-linear response of the MZM becomes worse. For Multi tone RoF-OFDM system, the variation of the received EVM with the RF modulation index is obtained with the input optical power to the photo detector kept constant at 1 dBm for each value of modulation index.

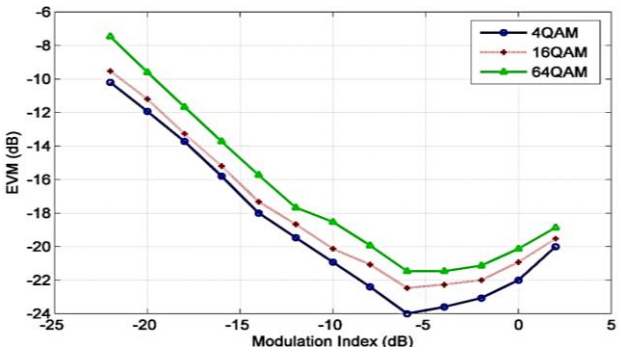

Fig. 11. EVM vs. Modulation Index for 80 Km SSMF Transmission

Fig. 11 shows the variation of the EVM with the RF modulation index of Mach Zhender Modulator (MZM). It is seen from the plot that value of EVM of each sub-band decreases when RF modulation index is increased until the optimum value of modulation index is reached (-6 dB). When RF Modulation index is further increased, the value of EVM gets increased, as the distortion induced by the inherent non-linear response of the MZM becomes worse which degrades the system performance.

5. Conclusions

The impact of various parameters including electrical power, RF modulation index of the MZM and received optical power on the system performance has been demonstrated by conducting theoretical, experimental and simulative analysis. The results of the multi-tone intermodulation analysis showed that at low values of RF modulation index, the power of the fundamental components is much higher than that of the IMD3 components. Increase in the RF modulation index results in the IMD3 components increasing faster than that of the fundamental. At an optimum value of modulation index (-7.5 dB), the power of the IMD3 component equals that of the fundamental. For values of modulation index greater than the optimum, the IMD3 distortion dominates and the system performance starts to degrade. Also, EVM of each sub-band decreases when RF modulation index is increased until the optimum value of modulation index is reached (-6.15 dB).

Acknowledgement

Facilities of experimental setup using Light Runner fiber optic and OSA available at CSIR-CSIO labs at Chandigarh are highly acknowledged by authors.

References

[1] V. Kamra, M. Kumar, Optik **122**(1), 44 (2011).
[2] S. Brindha, M. Meenakshi, J. Optoelectron. Adv. M. **9**(5-6), 855 (2015).
[3] T. Xia, R. Shetty, T. Platt, M. Slamani, J. Electron. Test **29**(6), 893 (2013).
[4] N. L'Esperance, T. Platt, M. Slamani, T. Xia, IEEE Transactions on Circuits and Systems II: Express Briefs **63**(6), 583 (2016).
[5] N. M. Devarajan, M. Chandrasekaran, J. Optoelectron. Adv. M., **9**(5-6), 561 (2015).
[6] M. Palanivelan, S. Anand, J. Optoelectron. Adv. M. **10(**11-12), 873 (2016).
[7] Y. Chu, R. Chakraborty, R. Friar, Z. Yang, IEEE International Symposium on Electromagnetic Compatibility (EMC), Ottawa, ON, 267 (2016).
[8] B. G. Kim, H. Kim, Y. C. Chung, J. Lightwave Technol. **35**(2), 145 (2017).
[9] Y. Y. Won, C. H. Kim, S. K. Han, D. Seo, Microw. Opt. Tech. Lett. **58**(11), 2662 (2016).
[10] H. J. Park, S. Y. Jung, S. H. Cho, J. H. Lee, S. K. Han, Microw. Opt. Tech. Lett. **58**(5), 1236 (2016).
[11] C. Viana et al., Electron. Lett. **51**(8), 640 (2015).
[12] S. Zhao, S. Cai, K. Kang, H. Qian, IEEE Global Conference on Signal and Information Processing (GlobalSIP), Orlando, FL, 1180 (2015).
[13] H. J. Park et al., IEEE Photonic. Tech. L. **28**(23), 2708 (2016).
[14] K. Freiberger, H. Enzinger, C. Vogel, IEEE Transactions on Microwave Theory and Techniques **PP**(99), 1 (2017).
[15] J. Guerreiro, R. Dinis, P. Montezuma, IEEE 82nd Vehicular Technology Conference (VTC2015-Fall), (2015).
[16] J. Wang, C. Liu, M. Zhu, M. Xu, Z. Dong, G. K. Chang, The European Conference on Optical Communication (ECOC), Cannes 1 (2014).
[17] R. B. Nunes, D. Coelho, J. A. L. Silva, M. E. V. Segatto, International Conference on Optical Network Design and Modeling, Stockholm 228 (2014).
[18] A. Kaur, K. S. Bhatia, A. Kaur, K. Singh, Optik **124**(22), 5747 (2013).
[19] Z. Zeng, M. Shao, 2018 International Conference on Sensor Networks and Signal Processing (SNSP), Xi'an, China, 13 (2018).
[20] H. J. Park, I. H. Ha, S-K Han, Opt. Commun. **144**, 160 (2019).
[21] R. Gupta, R. S. Kaler, Optoelectron. Adv. Mat. **12**(7-8), 441 (2018).
[22] T. H. Dahawi, Z. Yusoff, M. S. Salleh, J. M. Senior, IEEE 7th International Conference on Photonics (ICP), Kuah, 1 (2018).
[23] Y. Dong, R. P. Giddings, J. Tang, J. Lightwave Technol. **36**(23), 5640 (2018).
[24] M. Singh, J. Malhotra, Optoelectron. Adv. Mat. **13**(7-8), 437 (2019).
[25] P. Li et al., J. Lightwave Technol. **37**(4), 1424 (2019).

*Corresponding author: kamalbhatia.er@gmail.com